© 2022. Published by The Company of Biologists Ltd | Journal of Experimental Biology (2022) 225, jeb243572. doi:10.1242/jeb.243572

RESEARCH ARTICLE

Changes in apolipoprotein abundance dominate proteome responses to prolonged fasting in elephant seals

Jane I. Khudyakov[1,*], Rachel R. Holser[2], Craig A. Vierra[1], Serena T. Ly[1], Theron K. Niel[1], Basma M. Hasan[1], Daniel E. Crocker[3] and Daniel P. Costa[2]

ABSTRACT

Unlike many animals that reduce activity during fasting, northern elephant seals (NES) undergo prolonged fasting during energy-intensive life-history stages such as reproduction and molting, fueling fasting energy needs by mobilizing fat stores accrued during foraging. NES display several unique metabolic features such as high fasting metabolic rates, elevated blood lipid and high-density lipoprotein (HDL) cholesterol levels, efficient protein sparing and resistance to oxidative stress during fasting. However, the cellular mechanisms that regulate these adaptations are still not fully understood. To examine how metabolic coordination is achieved during prolonged fasting, we profiled changes in blubber, skeletal muscle and plasma proteomes of adult female NES over a 5 week fast associated with molting. We found that while blubber and muscle proteomes were remarkably stable over fasting, over 50 proteins changed in abundance in plasma, including those associated with lipid storage, mobilization, oxidation and transport. Apolipoproteins dominated the blubber, plasma and muscle proteome responses to fasting. APOA4, APOE and APOC3, which are associated with lipogenesis and triglyceride accumulation, decreased, while APOA1, APOA2 and APOM, which are associated with lipid mobilization and HDL function, increased over fasting. Our findings suggest that changes in apolipoprotein composition may underlie the maintenance of high HDL levels and, together with adipokines and hepatokines that facilitate lipid catabolism, may mediate the metabolic transitions between feeding and fasting in NES. Many of these proteins have not been previously studied in this species and provide intriguing hypotheses about metabolic regulation during prolonged fasting in mammals.

KEY WORDS: Blubber, Muscle, Plasma, Lipid mobilization, Lipid transport, proteomics

INTRODUCTION

Fasting is a natural and often predictable part of the life history of many animals. Prolonged fasting may be required for surviving periods of low food availability or be coupled to life-history stages such as migration, reproduction, hibernation and molting (Secor and Carey, 2016). Many animals that fast seasonally reduce energy needs during fasting periods by decreasing physical activity, metabolic rate and body temperature (Mohr et al., 2020). In contrast, capital-breeding and some migratory species forego food entirely during energetically demanding life-history stages. One capital-breeding mammal with remarkable fasting tolerance is the northern elephant seal (NES), *Mirounga angustirostris*. Because of the large distances between their pelagic foraging grounds and coastal rookeries, NES fast for several months during haul-out periods associated with breeding, lactation, molting and postnatal development on land (Champagne et al., 2012). Adult NES undergo two fasting periods per year. Adult males fast for up to 4 months during the breeding season while defending territories and breeding with females. Adult females fast for 4 weeks, during which they give birth and nurse their young with fat-rich milk. After a short post-breeding foraging trip, adults return to land to replace the entirety of their pelage in 4–5 weeks, a process known as catastrophic molt, while fasting (Holser, 2020; Worthy et al., 1992). As in other fasting-adapted animals, energy needs during fasting in NES are fueled by mobilization of large lipid stores that are accrued during foraging.

Many features of NES fasting metabolism have been described, such as high rates of fatty acid oxidation and endogenous glucose production, insulin resistance, and alterations in circulating corticosteroid, thyroid and adipokine hormones that may facilitate lipid catabolism and glucose and protein sparing (Fowler et al., 2018; Martinez et al., 2017; Rzucidlo et al., 2021). Unique features of NES metabolism that distinguish them from humans and laboratory mammals include extremely high fasting metabolic rates, efficient protein sparing despite elevated cortisol levels, low ketoacid production, maintenance of elevated high-density lipoprotein (HDL) levels, and resistance to oxidative stress during fasting (Crocker et al., 2014a; Ensminger et al., 2021; Tift et al., 2011). The endocrine, cellular and molecular mechanisms that underlie these features are not yet fully understood, and other unique metabolic adaptations are likely to be discovered, potentially via non-targeted and system-wide approaches (e.g. transcriptomics, proteomics).

A handful of studies have used such approaches to profile changes in global gene expression in response to fasting in NES tissues. They reported that genes encoding metabolic enzymes and extracellular matrix components were significantly downregulated in blubber and skeletal muscle during fasting, suggesting significant metabolic and structural reprogramming of tissues in response to food deprivation (Martinez et al., 2018; Wright et al., 2020). We also previously showed that experimental elevation of cortisol, which normally increases during fasting, resulted in altered expression of genes and abundance of proteins associated with insulin resistance, lipid metabolism, lipid droplet homeostasis and adipogenesis, among other functions, in NES blubber and skeletal muscle (Deyarmin et al., 2020, 2019; Khudyakov et al., 2017, 2015). However, more work is necessary to understand how these

[1]Biological Sciences Department, University of the Pacific, Stockton, CA 95211, USA. [2]Institute of Marine Sciences, University of California, Santa Cruz, CA 95064, USA. [3]Department of Biology, Sonoma State University, Rohnert Park, CA 94928, USA.

*Author for correspondence (jkhudyakov@pacific.edu)

J.I.K., 0000-0001-7038-102X; R.R.H., 0000-0002-8668-3839; C.A.V., 0000-0003-1889-819X; S.T.L., 0000-0002-2193-895X; T.K.N., 0000-0003-1279-6336; B.M.H., 0000-0002-5820-0780; D.E.C., 0000-0002-7940-8011; D.P.C., 0000-0002-0233-5782

Received 19 September 2021; Accepted 27 January 2022

Journal of Experimental Biology (2022) 225, jeb243572. doi:10.1242/jeb.243572

metabolic and cellular adjustments are coordinated within and across multiple tissues to maintain metabolic homeostasis during energy-intensive fasting periods in NES.

In this study, we examined the effects of fasting on the proteome – the functional output of the transcriptome – across three tissues to understand how metabolic coordination is achieved during prolonged fasting. We focused on blubber and skeletal muscle, the major source and sink of energy substrates, respectively, and plasma, which reflects the activity of the liver and other organs that cannot be easily sampled from free-ranging animals. We collected these tissues from five adult female NES at the beginning and end of a 5 week fasting period associated with catastrophic molting and compared protein abundance between early and late molt samples using label-free protein quantification by LC-MS/MS. We hypothesized that adipokines and enzymes associated with glucose oxidation and insulin signaling would decrease in abundance over fasting, while those associated with lipid catabolism and insulin resistance would increase. We found that the blubber and muscle proteomes remained remarkably stable, while over 50 proteins were differentially abundant in plasma over fasting. Apolipoproteins dominated the suite of proteins that responded to fasting, which also included adipokines and hepatokines associated with lipid mobilization, transport and catabolism. Many of the proteins that we identified have not been previously studied in NES, and lead to intriguing hypotheses about metabolic regulation during fasting that can be tested in future studies.

MATERIALS AND METHODS

Study animals

Samples were collected from adult female NES, *Mirounga angustirostris* (Gill 1866) (n=5), at Año Nuevo State Reserve (San Mateo County, CA, USA) during the May–June 2016 molting period. Animals were sampled within a few days of arrival at the rookery (early molt, 0% molted) and again several days before departure from the rookery (late molt, 100% molted). Two animals (5572 and 9678) were re-sampled upon returning to the rookery for breeding in January 2017. Animal metadata are shown in Table S1. All animal handling procedures were approved by the University of California, Santa Cruz, and Sonoma State University Institutional Animal Care and Use Committees and were conducted under National Marine Fisheries Service marine mammal permit no. 19108.

Sample collection

Study animals were chemically immobilized by intramuscular injection of Telazol (tiletamine/zolazepam HCl, Fort Dodge Labs) at a dosage of ∼1 mg kg^{-1} as described previously (Fowler et al., 2016; Robinson et al., 2012), and maintained with ∼25–50 mg bolus intravenous injections of Telazol. Blood samples were collected from the extradural vein into serum and EDTA-treated vacutainer tubes using an 18 gauge, 3.5 inch needle and chilled until return to the laboratory. Blood was centrifuged at 3000 ***g*** for 15 min at 4°C, and isolated serum and plasma were stored at −80°C. Blubber and muscle samples were collected from the posterior flank of each animal using a 6.0 mm diameter biopsy punch (Integra Miltex). Muscle samples were not obtained for one of the study animals (6762). Blubber samples were cut in half to separate outer (closest to skin) and inner (closest to muscle) layers, which were stored separately. Tissue samples were minced and incubated in RNA*later*™ Stabilization Solution (1.5 ml per ∼300 mg tissue; Invitrogen) and kept on ice until return to the laboratory. After 24 h of incubation at 4°C, RNA*later*™ was removed from blubber and muscle samples prior to storage at −80°C until further processing.

Mass was measured using a tripod, canvas sling and scale (±1 kg; MSI). Body composition (percent adiposity) was determined by the truncated cones method using morphometric and ultrasound measurements of blubber thickness (Gales and Burton, 1987). Adiposity was not obtained for animal 4448 at late molt. At the end of the procedure, seals received rear flipper tags (Dalton, Henley-on-Thames, Oxon, UK), and were allowed to recover from anesthesia and resume normal activity.

Protein extraction from blubber and muscle

Muscle and blubber tissues were processed to simultaneously extract protein and RNA. We used the inner half of each blubber sample in this study as this layer is considered more metabolically active than outer blubber in marine mammals (Ball et al., 2017; Struntz et al., 2004). Inner blubber tissue (∼100 mg) was minced with a sterile scalpel on dry ice and homogenized in 1 ml of Qiazol (Qiagen) by bead beating in a Bullet Blender Storm 24 instrument (Next Advance) for two cycles of 2 min each. Muscle tissue (∼50 mg) was processed similarly using 1 ml of Trizol (Invitrogen). Tissue homogenates were further disrupted using a 23 gauge needle and syringe. Following chloroform phase extraction, proteins were precipitated from the organic phase using isopropanol. Protein pellets were washed with 0.3 mol l^{-1} guanidine hydrochloride in 95% ethanol and stored at −20°C until further processing.

Sample preparation for mass spectrometry

Blubber and muscle protein pellets were resuspended in 200 µl of denaturing buffer [1% w/v sodium deoxycholate (SDC), 8 mol l^{-1} urea and 5 mmol l^{-1} dithiothreitol (DTT) in 50 mmol l^{-1} ammonium bicarbonate] by vortexing for 1 h at room temperature. Denaturing buffer was added to 5 µl plasma to a final volume of 200 µl. All samples were denatured for 1 h at 37°C, followed by alkylation with 15 mmol l^{-1} iodoacetamide in the dark at room temperature for 30 min. Alkylation was quenched with 5 mmol l^{-1} DTT. Samples were diluted with 50 mmol l^{-1} ammonium bicarbonate to reduce urea concentration to <1 mol l^{-1} and protein concentration was estimated using the Pierce BCA Protein Assay Kit (Thermo Scientific). Proteins were digested in solution using Pierce™ Trypsin Protease, MS Grade (Thermo Scientific) at 1:50 µg enzyme to protein ratio for 18 h at 37°C. Digested peptides were acidified to pH <2 using trifluoroacetic acid (TFA) to inactivate trypsin and precipitate SDC. Peptides were lyophilized, resuspended in 300 µl of 0.1% TFA, and desalted using Pierce™ Peptide Desalting Spin Columns (Thermo Scientific). Eluted peptides were lyophilized, resuspended in 0.1% formic acid in LC/MS-grade water, and quantified using Pierce™ Quantitative Colorimetric Peptide Assay (Thermo Scientific). Samples were assayed in duplicate [intra-assay coefficient of variation (CV) <3.0%, inter-assay CV <4.0%]. Peptide concentrations were determined using a quadratic fit for the standard curve (R^2=0.999) with Prism 8 software (GraphPad, USA).

LC-MS/MS

Peptide samples were diluted to 200 ng µl^{-1} with 0.1% formic acid in LC/MS-grade water and 5 µl were used per injection (with three injections per sample) for HPLC as described previously (Deyarmin et al., 2020). Mass spectrometry analyses were performed using an Orbitrap Fusion™ Tribrid™ mass spectrometer equipped with an EASY-Spray™ ion source (Thermo Fisher Scientific) operated in a data-dependent acquisition (DDA) manner by Xcalibur 4.0 software

(Thermo Fisher Scientific). MS1 spectra were resolved by the orbitrap with a resolution of 120,000, scan range of 200–1400 *m*/*z*, RF lens of 60%, AGC target of 1.0e6, and maximum injection time of 50 ms. Precursor ions selected using DDA were isolated by quadrupole and fragmented using higher-energy C-trap dissociation (HCD) with a collision energy of 28±3%. MS2 product ions were resolved by the orbitrap with resolution of 30,000, AGC target of 5.0e5, first mass of 100 *m*/*z*, and maximum injection time of 150 ms.

MS/MS data analyses

Protein identification and label-free quantification were performed using MaxQuant v1.6.14.0 with default settings. The 'match between runs' function was enabled with a matching time window of 0.7 min and an alignment time window of 20 min. Database search was conducted using MaxQuant's Andromeda search engine against the UniProtKB Caniformia database containing 509,245 entries (taxonomy ID: 379584, downloaded on 25 June 2020) and a MaxQuant contaminant database. Carbamidomethylation (C) was selected as a fixed modification and oxidation (M) and deamidation (NQ) were selected as variable modifications; a maximum of three modifications per peptide were allowed. False discovery rate (FDR) was determined by searching the reversed Caniformia and contaminant databases. Only hits below 1% FDR were retained for further analyses. Proteins with hits to contaminant or reversed databases and those with no unique peptides were removed. Protein quantification was conducted based on precursor ion intensity (median of 3 technical replicates) using the MaxLFQ algorithm in MaxQuant. Both razor and unique peptides were used for quantification and the minimum ratio for quantification was 2. FastLFQ normalization was used and the 'stabilize large LFQ ratios' and 'require MS/MS for LFQ comparisons' options were selected.

Lipid and hormone assays

Total cholesterol (TC), HDL and low-density lipoprotein/very low-density lipoprotein (LDL/VLDL) were measured in NES serum using EnzyChrom AF HDL and LDL/VLDL Assay Kit (BioAssay Systems, cat. no. E2HL-100, lot no. CA09A17). Serum samples were diluted 1:5 with assay buffer and run in duplicate (mean intra-assay CV=1.6%). Total triglyceride (TG) levels were measured in NES plasma using Triglyceride Colorimetric Assay Kit (Cayman Chemical, cat. no. 10010303, lot no. 0621449). Plasma samples were diluted 1:2 with standard diluent assay reagent and run in triplicate (mean intra-assay CV=2.3%). Cortisol levels in NES serum were measured using ELISA (Alpco, cat. no. 11-CORHU-E01, lot no. 202100). All samples were analyzed in duplicate (mean intra-assay CV=2.5%). Linearity of dilution was assessed using a series of six 1:2 dilutions of an NES serum sample with high cortisol levels. The slope of predicted versus measured values was 1.01 (R^2=0.99). Parallelism to the standard curve was assessed using log–logit transformation. The slopes of log–logit curves for diluted NES serum and the standard curve were not significantly different (NES serum: −0.62, standard curve: −0.59; ANCOVA: $F_{8,9}$=0.14, P=0.72). Assay accuracy was assessed by spiking NES serum samples with 10 and 60 µg dl^{-1} cortisol standards. The mean (±s.d.) recovery was 100.4±0.8%.

Statistical analyses

All statistical analyses were conducted using R v3.6.0 (http://www.R-project.org/). Pathway overrepresentation analyses of proteome data were conducted using the clusterProfiler package (Yu et al., 2012) against the human WikiPathways database version 20210510 (Slenter et al., 2018). Pathways were considered significantly enriched at Benjamini–Hochberg adjusted P<0.05 and q-value cutoff of 0.05. Protein expression was summarized using the pheatmap package (https://CRAN.R-project.org/package=pheatmap) with complete clustering of rows and columns by Euclidean distance. Principal components analyses (PCA) of protein expression were conducted using the prcomp function in the psych package (Revelle, 2019) and visualized using the factoextra package (https://CRAN.R-project.org/package=factoextra).

For differential protein abundance analyses, LFQ abundance values were $\log_2$-transformed, and proteins with >1 missing value per sample group were removed. The remaining missing values were imputed using the llsImpute function (k=150) in the pcaMethods package (Stacklies et al., 2007). Differential expression analyses were conducted using limma v3.40.6 (Ritchie et al., 2015) with blocking by subject to account for repeated sampling (design=∼Subject+Treatment). Proteins with abundances that differed by more than 20% between groups were considered differentially abundant at Benjamini–Hochberg-adjusted P<0.1.

Changes in mass, adiposity, cortisol, TG, TC, HDL and LDL/VLDL across fasting were assessed using linear mixed-effects models with fasting stage (levels=early, late) as a fixed effect and animal ID as a random effect using lme4 and lmerTest (Bates et al., 2015; Kuznetsova et al., 2017). Model residuals were assessed for normality using Shapiro–Wilk's test and visually to confirm model homoscedascity. Cortisol was log-transformed to achieve normality of model residuals.

RESULTS

We sampled five adult female NES twice during their spring fasting period associated with molting: within a week of arrival at the rookery (early molt) and at the completion of the molt, after 33±4 days (mean±s.d.) of fasting (late molt; Table S1). In addition, two of the five females were sampled again upon their return to the rookery for breeding from their post-molt foraging trip, 239 and 230 days after sampling during late molt (early breeding; Table S1). Females lost 27.8±3.9% of their body mass over the molt ($F_{1,3.1}$=252.22, P=0.00049; Fig. 1A; Table S1). Percentage body fat (adiposity) did not differ significantly between early and late molt ($F_{1,2.8}$=4.91, P=0.12; Fig. 1B; Table S1). The two females sampled after their post-molt foraging trip (during early breeding) had increased mass by 1.71-fold and 1.55-fold, with no appreciable change in adiposity (Table S1).

To examine molecular mechanisms operating during fasting and mass loss, we used LC-MS/MS to profile the proteomes of blubber, muscle and plasma collected early and late in the molting fast from the animals described above. We identified 1053 protein groups in blubber, 711 protein groups in muscle and 260 protein groups in plasma using the UniProt KB *Caniformia* database (Table S3). We first examined the functional composition of the proteomes as they have not been previously described in fasting NES. Pathways that were significantly enriched (adjusted P<0.05) in the inner blubber proteome included the VEGFA–VEGFR signaling pathway, cytoplasmic ribosomal proteins, complement system, proteasome degradation, electron transport chain, amino acid metabolism, glycolysis and gluconeogenesis, and Cori cycle, among others (Fig. 2A). Pathways enriched in the NES skeletal muscle proteome included the electron transport chain, cytoplasmic ribosomal proteins, striated muscle contraction pathway, glycolysis and gluconeogenesis, proteasome degradation, amino acid metabolism, fatty acid oxidation and TCA cycle, among others

Journal of Experimental Biology (2022) 225, jeb243572. doi:10.1242/jeb.243572

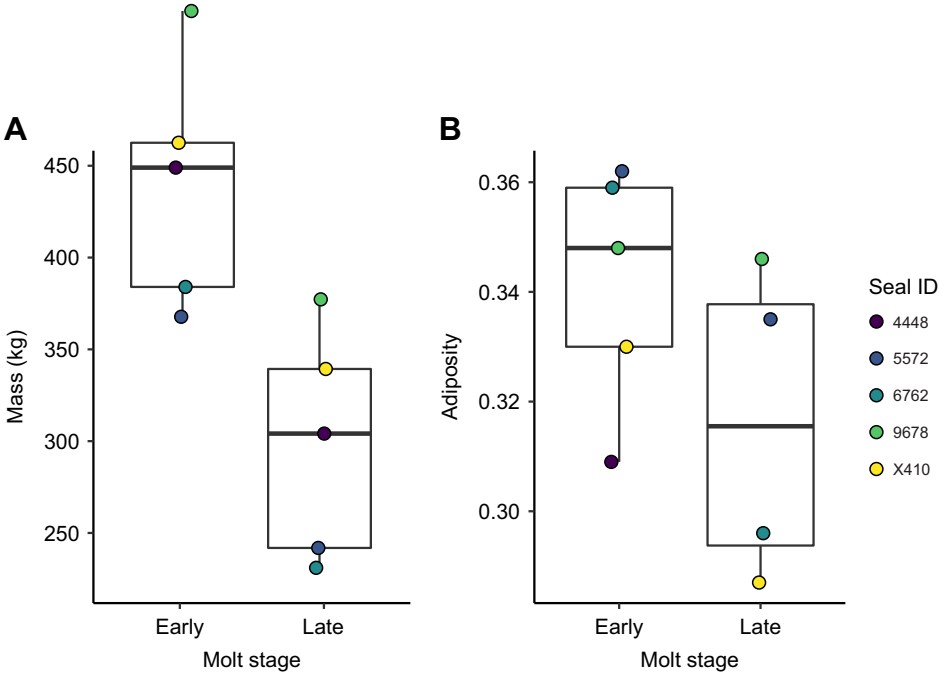

Fig. 1. Body mass and body fat of northern elephant seals during molt. Mass (A) and adiposity (B) of adult female northern elephant seals (NES; *n*=5) sampled at the beginning (early) and end (late) of their molting fast. Colors denote individual study animals. Adiposity was not obtained for one animal (4448) during late molt.

(Fig. 2B). Pathways enriched in the plasma proteome included complement and coagulation cascades, selenium micronutrient network, blood clotting cascade, folate metabolism, vitamin B12 metabolism, oxidative damage, composition of lipid particles, and metabolic pathway of LDL, HDL and TG, among others (Fig. 2C).

We next assessed whether protein abundance in each tissue was altered by fasting. After filtering out proteins with more than one missing value per sample group, we used 440 blubber proteins, 384 muscle proteins and 161 plasma proteins for differential protein abundance analyses (Table S4). Protein abundance in plasma, and to a lesser extent in muscle, varied by fasting stage, whereas protein abundance in blubber was not significantly affected by fasting (Fig. 3). Only two proteins in blubber – apolipoproteins A4 (APOA4) and E (APOE) – were identified as differentially abundant; both decreased over the molt (fold-change: APOE 0.19, APOA4 0.19; Fig. 4; Table S5). Five muscle proteins were differentially abundant between early and late fasting. Ferritin (FTL) abundance increased (fold-change: 4.82), while abundance of fructose-bisphosphate aldolase (ALDOA), LIM and cysteine-rich domains protein 1 (LMCD1), APOA4 and skeletal muscle troponin C (TNNC2) decreased over fasting (fold-change: TNNC2 0.08, APOA4 0.14, LMCD1 0.20, ALDOA 0.39; Fig. 4; Table S5).

The largest number of differentially abundant proteins (DAP; *n*=53) was detected in plasma, despite this tissue having the lowest number of identified proteins compared with the two others. The abundance of 29 plasma proteins increased, while 24 proteins decreased over fasting (Figs 4 and 5; Table S5). Plasma proteins that increased in abundance with fasting were associated with lipid and steroid transport (apolipoproteins APOA2, APOM and APOA1; corticosteroid-binding globulin, SERPINA6), lipid catabolism (zinc-alpha-2-glycoprotein, AZGP1; CD5 antigen-like, CD5L; properdin, CFP; pigment epithelium-derived factor, SERPINF1), adipogenesis (tetranectin, CLEC3B), complement system (e.g. complement C3), blood coagulation (e.g. coagulation factor F10), immune response and inflammation (e.g. immunoglobulin heavy chain constant mu, IGHM; beta-2-macroglobulin, B2M), biotin metabolism (biotinidase, BTD) and blood pressure regulation (angiotensinogen, AGT). Plasma proteins that decreased in abundance over fasting included apolipoproteins APOE, APOA4 and APOC3, acute phase proteins and hepatokines (alpha-2-macroglobulin, A2M; orosomucoid, ORM1; hemopexin, HPX; fetuin B, FETUB), coagulation factors (e.g. fibrinogen, FGA), proteins involved in iron and oxygen transport (serotransferrin, TF; hemoglobin subunit A, HBA), and the extracellular chaperone protein clusterin (CLU), among others (Figs 4 and 5; Table S5).

Lastly, we examined protein abundance in plasma samples obtained from two of the study animals upon their return to the rookery at the beginning of the breeding season, after over 7 months of foraging. Five plasma proteins increased in abundance over foraging (early breeding versus late molt): apolipoproteins APOE and APOA4, acute phase proteins ORM1 and ITIH4, and complement component C6 (fold-change: APOE 11.16, APOA4 3.86, ORM1 3.60, ITIH4 2.81, C6 1.96; Fig. 6; Table S5). Six proteins decreased in abundance over foraging: APOA1, albumin, coagulation factor F10, complement component C4A, and proteins associated with neutrophil degranulation (alpha-1B-glycoprotein, A1BG) and inflammation (attractin, ATRN; fold-change: F10 0.30, ATRN 0.41, C4A 0.47, A1BG 0.54, ALB 0.62, APOA1 0.63; Fig. 6; Table S5).

To assess the potential functional consequences of changes in abundance of proteins associated with cortisol and lipid transport over fasting and foraging, we measured circulating levels of cortisol, TG, TC, HDL and LDL/VLDL in the same animals. Cortisol levels increased by a mean of 11.90-fold over the molt ($F_{1,4.0}$=77.60, P=0.00092; Table S1) and decreased over foraging (0.62-fold and 0.88-fold). Total TG levels did not differ between early molt and late molt ($F_{1,4.0}$=0.48, P=0.52, Fig. 7A; Table S2), but increased between late molt and early breeding (2.13-fold and 1.26-fold). TC levels decreased by a mean of 0.89-fold over the molt ($F_{1,4.0}$=13.16, P=0.022; Fig. 7B; Table S2), but did not change appreciably over foraging (1.11-fold and 0.99-fold). HDL levels did not change significantly over fasting ($F_{1,4.0}$=4.10, P=0.11; Fig. 7C; Table S2). LDL/VLDL levels decreased marginally, by a mean of 0.82-fold, over the molt ($F_{1,4.0}$=6.57, P=0.062; Fig. 7D; Table S2). HDL and

Journal of Experimental Biology (2022) 225, jeb243572. doi:10.1242/jeb.243572

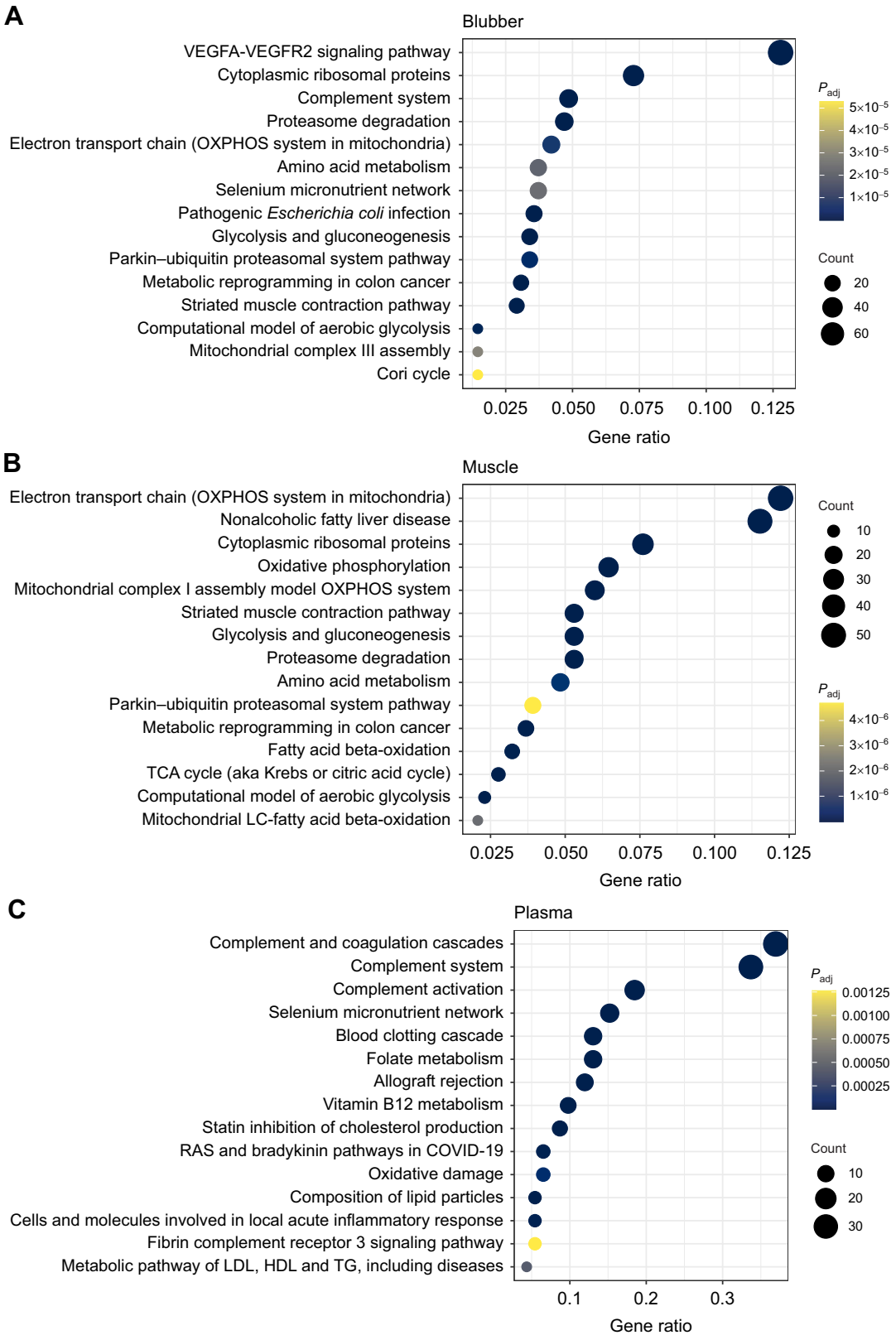

Fig. 2. Proteome profiles of blubber, muscle and plasma during molt. Metabolic pathways that were significantly overrepresented (adjusted P<0.05) in adult female NES blubber (A), skeletal muscle (B) and plasma (C) proteomes relative to the human proteome background. Overrepresentation analysis was conducted using Enrichr against the human WikiPathways database. Size of dots is scaled by the number of identified NES proteins mapping to each pathway, while color is scaled by adjusted P-value.

Journal of Experimental Biology (2022) 225, jeb243572. doi:10.1242/jeb.243572

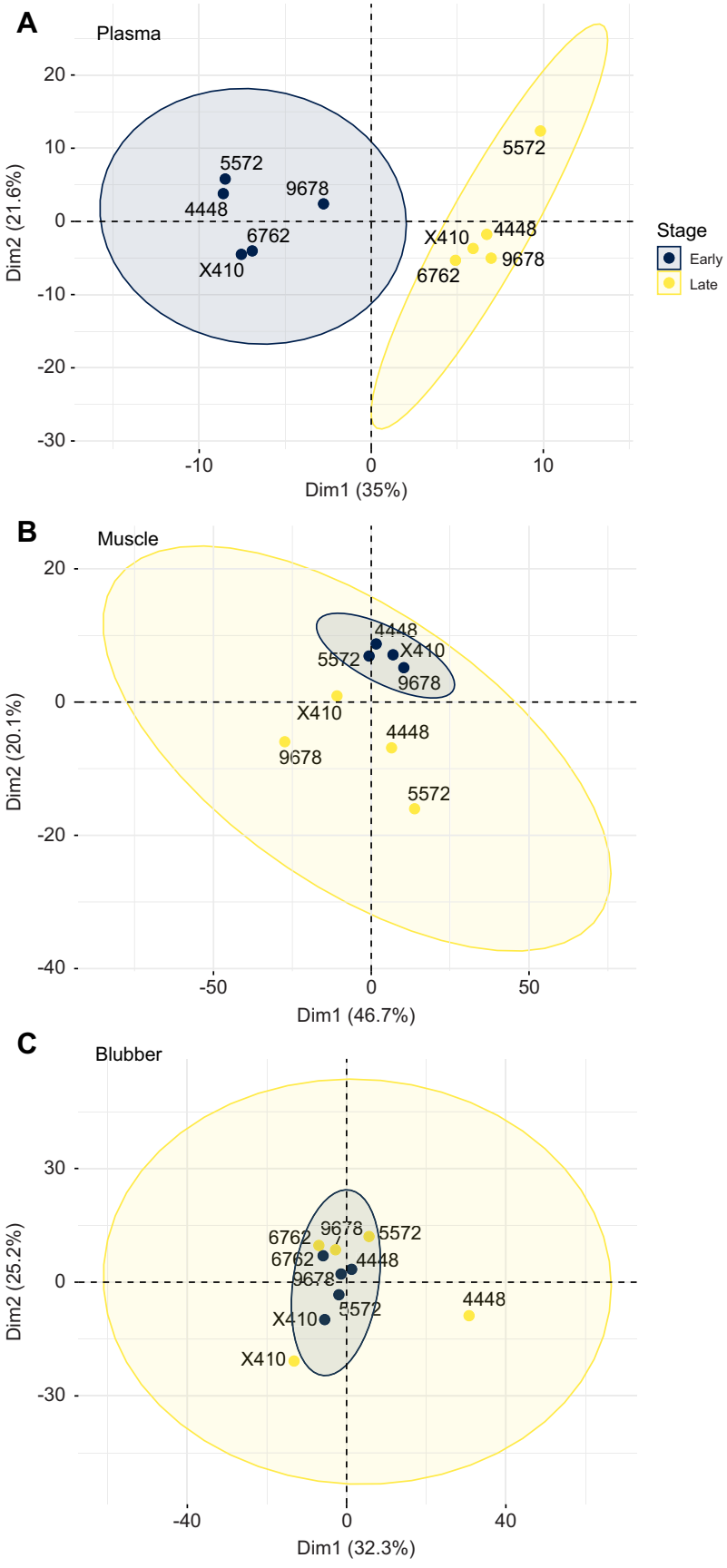

Fig. 3. Principal components analysis (PCA) plots of proteome data during molt. Plasma (A), skeletal muscle (B) and blubber (C) proteome data from adult female NES (*n*=5 for plasma and blubber, *n*=4 for muscle) sampled at the beginning (early) and end (late) of their molting fast. Ellipses show 95% confidence intervals for early and late molt sample groups.

Journal of Experimental Biology (2022) 225, jeb243572. doi:10.1242/jeb.243572

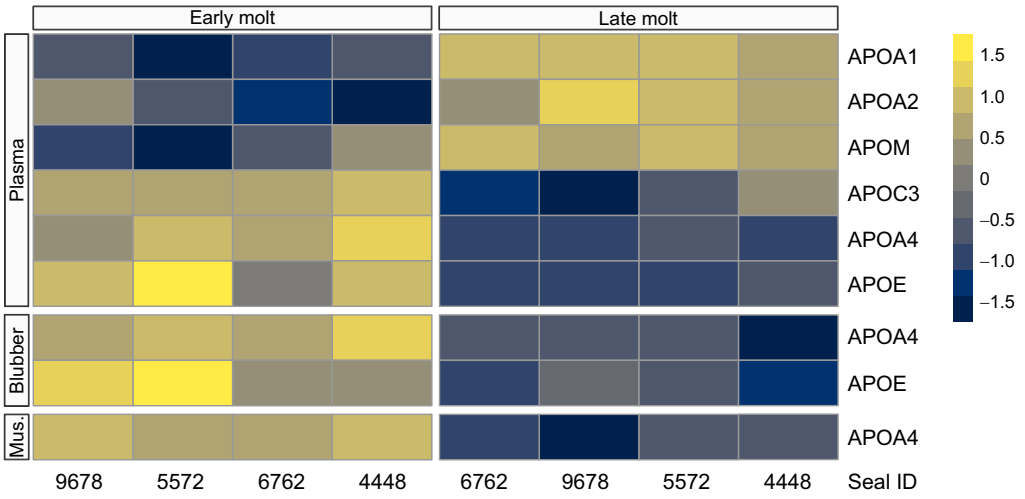

Fig. 4. Apolipoprotein abundance in plasma, muscle and blubber during molt. Heatmap showing $\log_2$-transformed and scaled abundance of apolipoproteins (rows) in plasma, blubber and skeletal muscle of adult female NES (n=4) sampled early and late in their molting fast. Columns were hierarchically clustered by Euclidean distance.

LDL/VLDL levels did not change consistently over foraging in the two animals sampled during early breeding (HDL: 0.88-fold and 1.07-fold; LDL/VLDL: 1.29-fold and 1.07-fold).

DISCUSSION

Capital-breeding marine mammals such as NES have adapted to undergo periods of foraging and fattening at sea followed by extended periods of complete fasting on land. The latter is remarkable in that elephant seals do not reduce energy expenditure during fasting. They maintain high rates of lipid oxidation and low rates of protein catabolism for its duration, which can last up to 4 months in breeding adult males (Champagne et al., 2012). Some of the endocrine and molecular mechanisms that regulate fasting metabolism in seals have been identified, including increases in corticosteroid and thyroid hormones, insulin resistance, alteration in adipokine signaling and expression of metabolic enzymes and transporters, and antioxidant defenses (Ensminger et al., 2021; Fowler et al., 2018; Rzucidlo et al., 2021). However, they have not been examined at the systems level in multiple tissues simultaneously. In this study, we used a non-targeted approach to identify changes in protein abundance across three tissues – blubber, muscle and plasma – over a fasting period associated with molting in adult female NES.

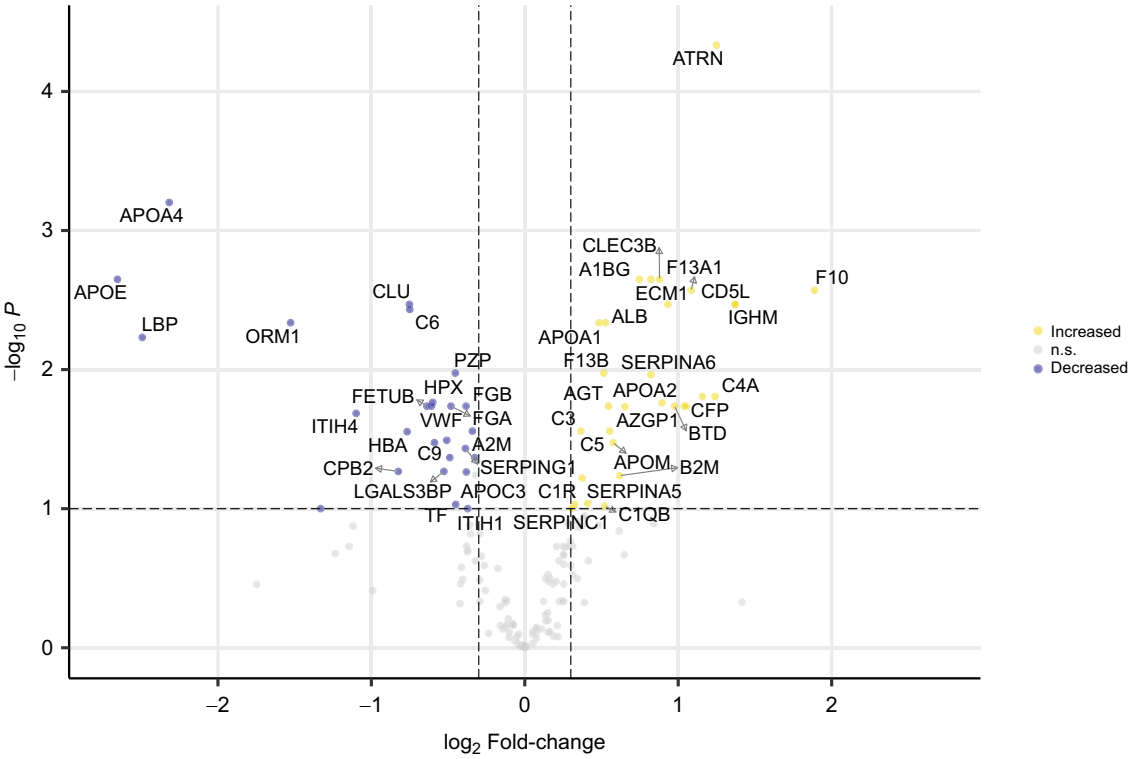

Fig. 5. Change in abundance of plasma proteins during molt. Volcano plot showing plasma proteins that were differentially abundant between early and late molt in adult female NES (n=5). Proteins that increased in abundance in late relative to early molt are shown in yellow, while those that decreased in abundance in late relative to early molt are shown in blue. Proteins shown in gray were not differentially abundant. Dashed lines show fold-change and P-value cutoffs (>20% change in abundance, adjusted P<0.01).

Journal of Experimental Biology (2022) 225, jeb243572. doi:10.1242/jeb.243572

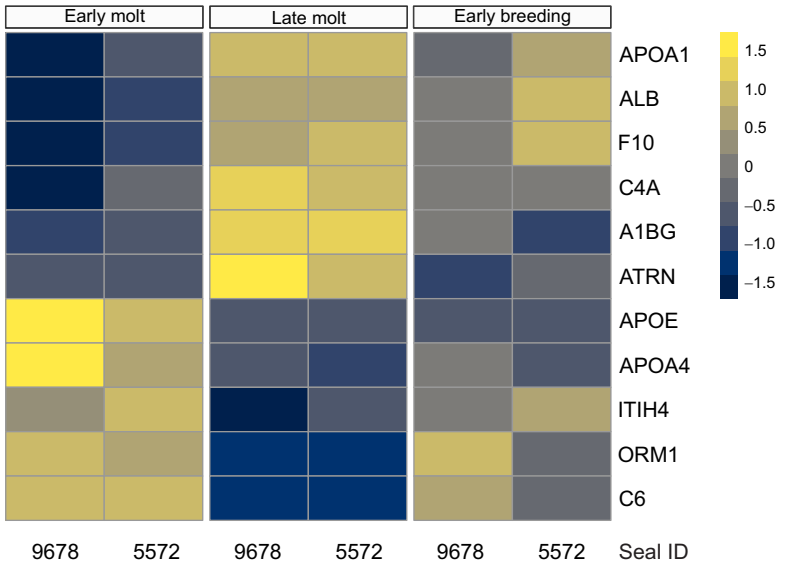

Fig. 6. Plasma protein abundance from molt to early breeding. Heatmap showing $\log_2$-transformed and scaled abundance of plasma proteins (rows) of two adult female NES sampled early and late in their molting fast (early molt, late molt) and upon return from a ∼9 month post-molting foraging trip (early breeding). Rows were hierarchically clustered by Euclidean distance.

Mass loss during fasting

Females lost a third of their body mass, or approximately 3 kg per day, during 5 weeks of fasting coupled with extremely rapid (‘catastrophic’) molting. However, body composition did not change significantly over the molt, as has been previously reported in this species (Worthy et al., 1992). Of the total mass lost by adult female NES during the molt, 41% has been attributed to fat, 14% to pelage, 25% to water and 20% to fat-free mass, which contributes additional water (Worthy et al., 1992; Wright et al., 2020). Water flux measurements have determined that over 90% of metabolic demands were met by lipid oxidation in molting seals, with some protein turnover serving to support rapid pelage synthesis (Worthy et al., 1992). We hypothesized that mechanisms that regulate fat-based metabolism and limit net protein loss during fasting would be reflected in proteomes of the main energy-provisioning and energy-utilizing tissues in NES.

Proteome analyses

We identified 1053 protein groups in blubber, 711 in muscle and 260 in plasma of fasting NES, many of which have not been previously studied in this species. Surprisingly, we found that NES blubber and muscle proteomes were remarkably stable over 28–37 days of fasting. This suggests that protein turnover in these tissues may be tightly controlled in a mammal adapted to prolonged fasting. Alternatively, the relatively high abundance of structural proteins, such as extracellular matrix components in blubber and contractile proteins in muscle, may have reduced the sensitivity of detection of metabolic enzymes and signaling molecules, which are produced in lower abundance. A small sample size and high individual variability also constrained our power to detect additional differences between early and late fasting in muscle and blubber. Despite these limitations, we detected highly consistent changes in apolipoprotein abundance across three tissues and identified over 50 differentially abundant proteins in the plasma of fasting seals (Fig. 8).

Skeletal muscle response to fasting

The proteins that were differentially abundant over fasting in skeletal muscle of NES suggest metabolic and structural adjustments to fasting and inactivity and putative protective mechanisms against oxidative damage. The sole protein that increased in abundance in muscle during fasting was FTL. This transport protein sequesters free iron inside cells to prevent the generation of reactive oxygen species (Halon-Golabek et al., 2019). FTL may be a key component of antioxidant defense in seal muscle, which has some of the largest myoglobin stores, and thus iron content, in mammals (Hassrick et al., 2010). Studies in mice have also shown that impairment of the insulin signaling pathway or treatment with adiponectin causes an upregulation of FTL, increasing cellular resistance to oxidative stress (Halon-Golabek et al., 2019; Ikegami et al., 2009). We hypothesize that the increase in FTL abundance, potentially due to insulin resistance, may contribute to the remarkable tolerance to oxidative damage in fasting seals (Ensminger et al., 2021). Muscle proteins that decreased in abundance during fasting included ALDOA, LMCD1 and TNNC2. *ALDOA* transcripts were also downregulated in the muscle of the same animals over fasting (Wright et al., 2020), suggesting that this glycolytic enzyme may be regulated, in part, at the transcriptional level. Aldolase downregulation may play a role in shifting substrate utilization from carbohydrates to lipids and is consistent with the decrease in glucose oxidation reported in late-fasted NES (Houser et al., 2012). LMCD1 is a positive regulator of muscle mass that stimulates protein synthesis by activating IRS1 and AKT (Ferreira et al., 2019), which decrease during fasting in NES (Viscarra et al., 2011). A decrease in LMCD1 abundance may serve to limit protein synthesis in muscle during molting in order to preserve amino acids for skin and hair growth. TNNC2, a sarcoplasmic protein that regulates muscle contraction, increases in abundance in response to exercise in humans (Vann et al., 2020), and decreases in abundance during fasting in fish (Zhang et al., 2021). Its decline in seal muscle during fasting is consistent with reduced activity during terrestrial molting (compared with foraging) in NES. Together, these data suggest potential shifts in carbohydrate metabolism, antioxidant defenses and energy-sparing mechanisms in NES muscle during fasting.

Apolipoprotein dynamics during fasting and feeding

Alterations in apolipoprotein abundance dominated blubber, plasma and muscle proteome responses to fasting and the plasma response to feeding. Apolipoproteins associated with lipogenesis and TG accumulation (APOA4, APOE, APOC3) decreased, while those associated with lipid mobilization and HDL function

Journal of Experimental Biology (2022) 225, jeb243572. doi:10.1242/jeb.243572

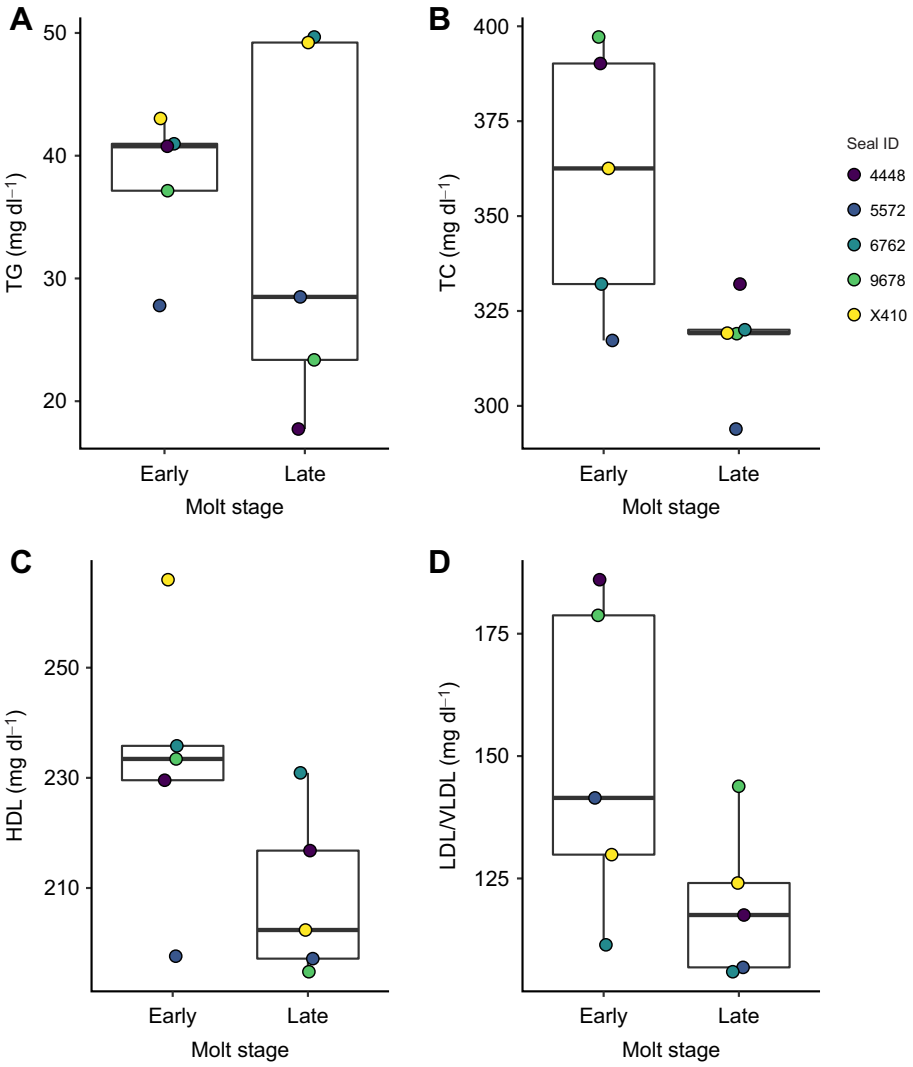

Fig. 7. Abundance of circulating lipids during molt. Plasma triglycerides (TG; A), serum total cholesterol (TC; B), serum high-density lipoprotein (HDL; C) and serum low-density lipoprotein and very low-density lipoprotein (LDL/VLDL; D) measured in adult female NES (*n*=5) at the beginning (early) and end (late) of their molting fast. Colors denote individual study animals.

(APOA1, APOA2, APOM) increased over fasting in NES. Apolipoproteins AIV and E emerged as the most definitive markers of nutritional state in NES. Their abundance decreased in plasma and blubber over fasting and increased in plasma after foraging. APOA4 also declined in skeletal muscle over fasting. In mice and humans, APOA4 is expressed primarily by enterocytes of the small intestine in response to lipid ingestion (Su and Peng, 2020); its expression in other tissues has not been described. It mediates chylomicron assembly in the small intestine and stimulates lipid uptake into cells by increasing the activity of lipoprotein lipase (LPL) (Qu et al., 2021; Zhu et al., 2020). APOA4 levels increase with feeding and decrease with fasting in mice (Wang et al., 2015), similar to our NES results. Recent studies have shown that APOA4 is also involved in stimulating insulin secretion, promoting glucose uptake by peripheral tissues via the PI3K–Akt pathway, inhibiting hepatic gluconeogenesis, and suppressing food intake (Li et al., 2017; Qu et al., 2019; Wang et al., 2015). Its decrease during fasting in NES may contribute to glucose sparing during prolonged fasting and is consistent with the hypoinsulinemia, insulin resistance, a high rate of endogenous glucose production and a fasting-associated decrease in Akt phosphorylation described in this species (Fowler et al., 2018; Viscarra et al., 2011). A decline in APOA4 levels across multiple tissues may also serve as one of the orexigenic signals for departure from the rookery at the end of the fast.

APOE, a major component of VLDL, is expressed in liver and adipose tissue and has been shown to mediate triglyceride accumulation, lipogenesis and adipogenesis in humans and mice (Su and Peng, 2020). *APOE* expression increases in response to a high-fat diet and decreases in response to caloric restriction and fasting in mice (Huang et al., 2007). Specific APOE ablation in mouse adipose tissue enhances lipolysis, fatty acid oxidation and insulin sensitivity, and increases the expression of adiponectin, an adipokine that stimulates fatty acid catabolism (Jiang et al., 2021). Our previous work showed that adiponectin expression in blubber increases over the molting fast in adult female NES (Khudyakov et al., 2019). A decline in APOE levels over fasting may contribute to adiponectin upregulation and the high rates of lipid catabolism seen in fasting NES (Fowler et al., 2018). While a higher abundance of APOE in early fasting may promote insulin resistance, decreased levels in late fasting may increase insulin sensitivity in preparation for foraging and fattening at sea. In contrast, an increase in APOE (and APOA4) abundance over foraging likely facilitates fat deposition and accumulation.

APOC3 levels decreased, while APOA1, APOA2 and APOM increased in plasma over fasting. In contrast, APOA1 abundance decreased after foraging. APOC3, a constituent of VLDL, is a known inhibitor of LPL and lipolysis of triglyceride-rich lipoproteins in humans (Borén et al., 2020). *APOC3* overexpression in mice

Journal of Experimental Biology (2022) 225, jeb243572. doi:10.1242/jeb.243572

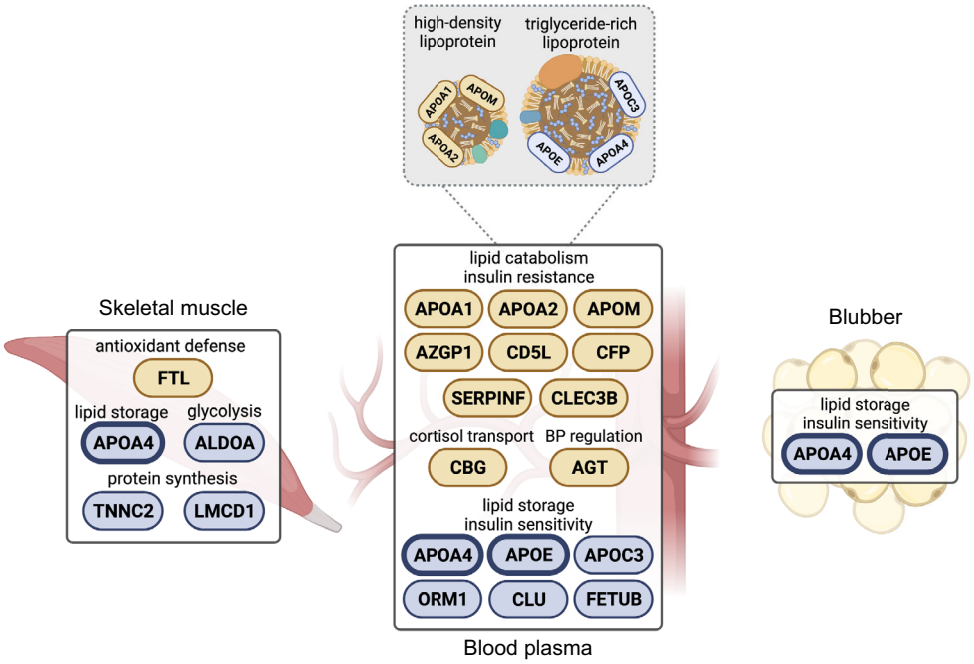

Fig. 8. Summary of differentially abundant proteins (DAP) that were identified in adult female NES over 5 weeks of fasting. Skeletal muscle (left), blood plasma (center; not all plasma DAP are shown) and blubber (right). DAP that increased in abundance over fasting are shown in yellow, while those that decreased are shown in blue. Putative functions of DAP were inferred from the literature. DAP that were identified in multiple tissues are indicated by a bold outline. Together, changes in protein abundance likely facilitate lipid catabolism and insulin resistance during fasting. Triglyceride-rich lipoprotein: chylomicron, VLDL. BP, blood pressure. Created with BioRender.com.

stimulates *de novo* lipogenesis and VLDL production, while its loss of function results in reduced TG accumulation (Su and Peng, 2020). APOA1, APOA2 and APOM are HDL components associated with lipid turnover in mice and humans. APOA1 upregulates lipases and increases fatty acid oxidation, while APOM inhibits TG uptake by adipose tissue and promotes insulin resistance; both reduce hepatic TG accumulation (Christoffersen et al., 2018; Hajny et al., 2021; Su and Peng, 2020). *APOM* expression in adipose tissue increases with caloric restriction, and decreases with obesity in humans (Sramkova et al., 2019), similar to our findings in NES. Lastly, APOA2 has been positively correlated with circulating free fatty acid levels and insulin resistance in humans (Weng and Breslow, 1996). Together, the alterations in apolipoproteins described in this study suggest additional mechanisms that regulate lipid metabolism and sensitivity to insulin in fasting and feeding NES (Fowler et al., 2018). Specifically, apolipoproteins likely contribute to suppression of lipogenesis and maintenance of high levels of lipid mobilization during fasting.

Plasma response to fasting

Other plasma proteins that responded to fasting in NES have known roles in lipid metabolism. Those that increased in abundance over fasting included cytokines, adipokines and complement proteins associated with lipid catabolism and insulin resistance (CD5L, AZGP1, SERPINF, CFP, CLEC3B), while those that decreased were associated with lipid storage, adipogenesis, obesity and insulin sensitivity (ORM1, HPX, FETUB, CLU). ORM1 was also one of the proteins that increased in abundance over foraging. CD5L (AIM), the second most highly increased protein in plasma, is a cytokine produced by adipose tissue-associated macrophages that stimulates lipolysis and decreases lipid droplet size by inhibiting fatty acid synthase in mice (Kurokawa et al., 2010). AZGP1 and SERPINF are adipokines that promote lipolysis and insulin resistance in mice and humans (Huang et al., 2018; Wei et al., 2019). Circulating AZGP1 levels in humans are correlated with IgM (Wei et al., 2019), which also increased in abundance over fasting in NES. The complement protein CFP inhibits fatty acid uptake and TG synthesis in mouse adipocytes (Gauvreau et al., 2012). In contrast, the acute phase protein ORM1 inhibits lipolysis and promotes insulin sensitivity in mice (Lee et al., 2010). HPX is a heme-scavenging plasma protein that increases in response to a high-fat diet and stimulates adipogenesis in mice (Lawson et al., 2017). The hepatokine FETUB is associated with liver steatosis in humans (Meex et al., 2015). CLU is a molecular chaperone of secreted proteins that is positively associated with adiposity and liver steatosis and negatively associated with APOA1 levels in humans and mice (Wittwer and Bradley, 2021). Together, lipolysis during fasting in NES may be stimulated, in part, by an increase in abundance of pro-lipolytic factors such as AZGP1 and a decrease in abundance of anti-lipolytic proteins such as ORM1. Lipid mobilization may also be facilitated by a reduction in abundance of lipogenic factors such as CLU. In contrast, an increase in ORM1 abundance during foraging likely facilitates lipid storage.

Other differentially abundant plasma proteins of interest included SERPINA6 (CBG) and AGT, which increased over fasting. Cortisol increases across most NES haul-out periods and may promote the high rates of lipolysis that characterize fasting in this species (Crocker et al., 2014b). Cortisol also increased significantly over fasting in this study; a parallel increase in CBG levels across fasting may regulate accessibility of this hormone, which has significant impacts on immune and reproductive function, to some tissues (Sapolsky et al., 2000). An increase in CBG at the end of the molting fast in adult female NES may facilitate embryo implantation by buffering reproductive tissues from prolonged exposure to high cortisol levels. AGT is produced by the liver, adipose tissue and kidneys and serves as the substrate for the renin–angiotensin–aldosterone system (RAAS), which regulates blood pressure (Lu et al., 2016). The increase in circulating AGT over the molt in adult female NES was consistent with previous work showing that Ang II, another component of the RAAS, increased across fasting in adult males (Ortiz et al., 2006). In contrast, adipose, muscle and plasma AGT levels decreased during fasting in weaned NES pups (Suzuki et al., 2013). The discrepancy between our data and that of Suzuki

et al. (2013) may be explained by differences in physiology between pups and adults as well as differences in sensitivity of analytical methods (LC-MS/MS versus western blot). While increases in AGT and other RAAS components may serve to maintain plasma volume and osmolarity during fasting, they have recently been implicated in obesity, insulin resistance and inflammation in humans and laboratory systems (Lu et al., 2016). Further work will be necessary to untangle the role of this system in marine mammal fasting physiology.

Changes in circulating lipids during fasting

Coincident with changes in apolipoprotein abundance, we found that TC and VLDL/LDL concentrations significantly declined, while HDL and TG levels were unaffected by fasting in adult female NES. Other studies of molting females have shown that TG levels do not decrease significantly over fasting, presumably because of a high rate of fatty acid re-esterification, which is typical in fasting mammals (Crocker et al., 2014a; Fowler et al., 2016). Similar effects of fasting on lipid profiles have been reported for adult male NES, although a decrease in TC and LDL levels was only noted during breeding, but not during the molting fast (Tift et al., 2011). In mice, fasting decreases the expression of enzymes involved in cholesterol synthesis by downregulating the transcription factors *SREBP1* and *SREBP2* (Horton et al., 1998). The decrease in TC levels observed in fasting NES may result from a similar reduction in cholesterol synthesis. The marginal decrease in VLDL/LDL levels observed in this study may be attributed to cholesterol mobilization for steroidogenesis, as corticosteroid levels generally increase over fasting in NES (Fowler et al., 2018). In addition, delayed implantation of an egg fertilized at the end of the previous breeding season is thought to occur at some point during the molting fast (Ling and Thomas, 1967), which would necessitate increased synthesis of progesterone. In contrast, HDL was maintained at high levels during the molting fast in adult female NES, similar to males, potentially as a protective mechanism against oxidative stress associated with prolonged fasting and sleep apneas on land (Brites et al., 2017; Ensminger et al., 2021). We propose that an increase in abundance of APOA1, APOA2 and APOM over fasting may contribute to the maintenance of high HDL levels and its antioxidant properties in NES (Brites et al., 2017).

Conclusions

This study is the first to use LC-MS/MS to examine changes in protein abundance in multiple tissues over prolonged fasting in a free-ranging marine mammal. While the blubber and muscle proteomes were surprisingly stable over fasting, we identified changes in abundance of many circulating proteins that are secreted by the liver and other tissues which cannot be easily sampled from free-ranging marine mammals. Our findings suggest that changes in abundance of a suite of apolipoproteins, adipokines and hepatokines may underlie metabolic transitions between feeding and fasting. These changes include a decrease in the abundance of proteins associated with lipogenesis and an increase in the abundance of proteins associated with lipid catabolism over fasting. Together, these data provide insights into metabolic regulation during prolonged fasting in mammals, as well as protein sequence data for further studies in marine mammals.

Acknowledgements

We are grateful to Elizabeth McHuron, Patrick Robinson and Luis Huckstadt for their assistance with sample collection and the rangers at Año Nuevo State Park for providing access to study animals. We would like to thank Rasool Maan, Melony Mody and Reeti Banerjee for help with sample processing and Kieu Diem Nguyen, Christina Tang and Edrick Tan for assistance with data analyses. We also thank Jessica Avalos and Anna Keith for their assistance with cortisol assays and validation.

Competing interests

The authors declare no competing or financial interests.

Author contributions

Conceptualization: J.I.K.; Methodology: R.R.H., C.A.V.; Validation: J.I.K.; Formal analysis: J.I.K., R.R.H., C.A.V., S.T.L., T.K.N., B.M.H., D.E.C.; Investigation: J.I.K.; Resources: R.R.H., C.A.V., D.P.C.; Data curation: J.I.K., R.R.H., C.A.V., S.T.L., T.K.N., B.M.H.; Writing - original draft: J.I.K.; Writing - review & editing: R.R.H., S.T.L., T.K.N., B.M.H., D.E.C., D.P.C.; Visualization: J.I.K., S.T.L., T.K.N., B.M.H.; Supervision: J.I.K., D.P.C.; Project administration: J.I.K.; Funding acquisition: J.I.K., D.P.C.

Funding

Funding was provided in part by the University of the Pacific (Pacific Fund and College Research Fund grants to J.I.K.). Field logistics was supported by awards to D.P.C. from the E&P Sound and Marine Life Joint Industry Programme (JIP) of the International Association of Oil and Gas Producers (IOGP) (grant no. 00-07-23) and the Office of Naval Research (ONR) (grant no. N00014-18-1-2822).

Data availability

The raw data and MaxQuant output files generated during this study are available at ProteomeXchange MassIVE repository (doi:10.25345/C5225Q).

References

Ball, H. C., Londraville, R. L., Prokop, J. W., George, J. C., Suydam, R. S., Vinyard, C., Thewissen, J. G. and Duff, R. J. (2017). Beyond thermoregulation: metabolic function of cetacean blubber in migrating bowhead and beluga whales. *J. Comp. Physiol. B* **187**, 235-252. doi:10.1007/s00360-016-1029-6

Bates, D., Mächler, M., Bolker, B. and Walker, S. (2015). Fitting linear mixed-effects models using lme4. *J. Stat. Softw.* **67**, 48. doi:10.18637/jss.v067.i01

Borén, J., Packard, C. J. and Taskinen, M.-R. (2020). The roles of ApoC-III on the metabolism of triglyceride-rich lipoproteins in humans. *Front. Endocrinol.* **11**, 474. doi:10.3389/fendo.2020.00474

Brites, F., Martin, M., Guillas, I. and Kontush, A. (2017). Antioxidative activity of high-density lipoprotein (HDL): Mechanistic insights into potential clinical benefit. *BBA clinical* **8**, 66-77. doi:10.1016/j.bbacli.2017.07.002

Champagne, C. D., Crocker, D. E., Fowler, M. A. and Houser, D. S. (2012). Fasting physiology of the pinnipeds: the challenges of fasting while maintaining high energy expenditure and nutrient delivery for lactation. In *Comparative Physiology of Fasting, Starvation, and Food Limitation* (ed. M. D. McCue), pp. 309-336. Springer.

Christoffersen, C., Federspiel, C. K., Borup, A., Christensen, P. M., Madsen, A. N., Heine, M., Nielsen, C. H., Kjaer, A., Holst, B., Heeren, J. et al. (2018). The apolipoprotein M/S1P axis controls triglyceride metabolism and brown fat activity. *Cell Reports* **22**, 175-188. doi:10.1016/j.celrep.2017.12.029

Crocker, D. E., Champagne, C. D., Fowler, M. A., Houser, D. S. (2014a). Adiposity and fat metabolism in lactating and fasting northern elephant seals. *Adv Nutr* **5**, 57-64. doi:10.3945/an.113.004663

Crocker, D. E., Fowler, M. A., Champagne, C. D., Vanderlugt, A. L. and Houser, D. S. (2014b). Metabolic response to a glucagon challenge varies with adiposity and life-history stage in fasting northern elephant seals. *Gen. Comp. Endocrinol.* **195**, 99-106. doi:10.1016/j.ygcen.2013.11.005

Deyarmin, J., Hekman, R., Champagne, C., McCormley, M., Stephan, A., Crocker, D., Houser, D. and Khudyakov, J. (2020). Blubber proteome response to repeated ACTH administration in a wild marine mammal. *Comp. Biochem. Physiol. D Genomics Proteomics* **33**, 100644. doi:10.1016/j.cbd.2019.100644

Deyarmin, J. S., McCormley, M. C., Champagne, C. D., Stephan, A. P., Pujade Busqueta, L., Crocker, D. E., Houser, D. S. and Khudyakov, J. I. (2019). Blubber transcriptome responses to repeated ACTH administration in a marine mammal. *Sci. Rep.* **9**, 2718. doi:10.1038/s41598-019-39089-2

Ensminger, D. C., Salvador-Pascual, A., Arango, B. G., Allen, K. N. and Vázquez-Medina, J. P. (2021). Fasting ameliorates oxidative stress: a review of physiological strategies across life history events in wild vertebrates. *Comp. Biochem. Physiol. A Mol. Integr. Physiol.* **256**, 110929. doi:10.1016/j.cbpa.2021.110929

Ferreira, D. M. S., Cheng, A. J., Agudelo, L. Z., Cervenka, I., Chaillou, T., Correia, J. C., Porsmyr-Palmertz, M., Izadi, M., Hansson, A., Martínez-Redondo, V. et al. (2019). LIM and cysteine-rich domains 1 (LMCD1) regulates skeletal muscle hypertrophy, calcium handling, and force. *Skeletal Muscle* **9**, 26. doi:10.1186/s13395-019-0214-1

Fowler, M. A., Debier, C., Champagne, C. D., Crocker, D. E. and Costa, D. P. (2016). The demands of lactation promote differential regulation of lipid stores in

fasting elephant seals. *Gen. Comp. Endocrinol.* **225**, 125-132. doi:10.1016/j.ygcen.2015.09.024
Fowler, M. A., Champagne, C. D. and Crocker, D. E. (2018). Adiposity and fat metabolism during combined fasting and lactation in elephant seals. *J. Exp. Biol.* **221**, jeb161554. doi:10.1242/jeb.161554
Gales, N. J. and Burton, H. R. (1987). Ultrasonic measurement of blubber thickness of the southern elephant seal, mirounga-leonina (Linn). *Aust. J. Zool.* **35**, 207-217. doi:10.1071/ZO9870207
Gauvreau, D., Roy, C., Tom, F. Q., Lu, H., Miegueu, P., Richard, D., Song, W. C., Stover, C. and Cianflone, K. (2012). A new effector of lipid metabolism: complement factor properdin. *Mol. Immunol.* **51**, 73-81. doi:10.1016/j.molimm.2012.02.110
Hajny, S., Borup, A., Elsøe, S. and Christoffersen, C. (2021). Increased plasma apoM levels impair triglyceride turnover in mice. *Biochim. Biophys. Acta Mol. Cell Biol. Lipids* **1866**, 158969. doi:10.1016/j.bbalip.2021.158969
Halon-Golabek, M., Borkowska, A., Herman-Antosiewicz, A. and Antosiewicz, J. (2019). Iron Metabolism of the Skeletal Muscle and Neurodegeneration. *Front. Neurosci.* **13**, 165. doi:10.3389/fnins.2019.00165
Hassrick, J. L., Crocker, D. E., Teutschel, N. M., McDonald, B. I., Robinson, P. W., Simmons, S. E. and Costa, D. P. (2010). Condition and mass impact oxygen stores and dive duration in adult female northern elephant seals. *J. Exp. Biol.* **213**, 585-592. doi:10.1242/jeb.037168
Holser, R. R. (2020). A top predator in hot water: Effects of a marine heatwave on foraging and reproduction in the northern elephant seal. *Doctoral dissertation*, University of California Santa Cruz. ProQuest Dissertations Publishing.
Horton, J. D., Bashmakov, Y., Shimomura, I. and Shimano, H. (1998). Regulation of sterol regulatory element binding proteins in livers of fasted and refed mice. *Proc. Natl Acad. Sci. USA* **95**, 5987. doi:10.1073/pnas.95.11.5987
Houser, D. S., Crocker, D. E., Tift, M. S. and Champagne, C. D. (2012). Glucose oxidation and nonoxidative glucose disposal during prolonged fasts of the northern elephant seal pup (Mirounga angustirostris). *Am. J. Physiol. Regul. Integr. Comp. Physiol.* **303**, R562-R570. doi:10.1152/ajpregu.00101.2012
Huang, Z. H., Luque, R. M., Kineman, R. D. and Mazzone, T. (2007). Nutritional regulation of adipose tissue apolipoprotein E expression. *Am. J. Physiol. Endocrinol. Metab.* **293**, E203-E209. doi:10.1152/ajpendo.00118.2007
Huang, K.-T., Lin, C.-C., Tsai, M.-C., Chen, K.-D. and Chiu, K.-W. (2018). Pigment epithelium-derived factor in lipid metabolic disorders. *Biomed. J.* **41**, 102-108. doi:10.1016/j.bj.2018.02.004
Ikegami, Y., Inukai, K., Imai, K., Sakamoto, Y., Katagiri, H., Kurihara, S., Awata, T. and Katayama, S. (2009). Adiponectin upregulates ferritin heavy chain in skeletal muscle cells. *Diabetes* **58**, 61-70. doi:10.2337/db07-0690
Jiang, C.-L., Chen, Y.-F. and Lin, F.-J. (2021). Apolipoprotein E deficiency activates thermogenesis of white adipose tissues in mice through enhancing β-hydroxybutyrate production from precursor cells. *FASEB J.* **35**, e21760.
Khudyakov, J. I., Champagne, C. D., Preeyanon, L., Ortiz, R. M. and Crocker, D. E. (2015). Muscle transcriptome response to ACTH administration in a free-ranging marine mammal. *Physiol. Genomics* **47**, 318-330. doi:10.1152/physiolgenomics.00030.2015
Khudyakov, J. I., Champagne, C. D., Meneghetti, L. M. and Crocker, D. E. (2017). Blubber transcriptome response to acute stress axis activation involves transient changes in adipogenesis and lipolysis in a fasting-adapted marine mammal. *Sci. Rep.* **7**, 42110. doi:10.1038/srep42110
Khudyakov, J. I., Eileen Abdollahi, E., Angela Ngo, A., Sandhu, G., Stephan, A., Costa, D. P. and Crocker, D. E. (2019). Expression of obesity-related adipokine genes during fasting in a naturally obese marine mammal. *Am. J. Physiol. Integr. Comp. Physiol.* **317**, R521-R529. doi:10.1152/ajpregu.00182.2019
Kurokawa, J., Arai, S., Nakashima, K., Nagano, H., Nishijima, A., Miyata, K., Ose, R., Mori, M., Kubota, N., Kadowaki, T. et al. (2010). Macrophage-derived AIM is endocytosed into adipocytes and decreases lipid droplets via inhibition of fatty acid synthase activity. *Cell Metab.* **11**, 479-492. doi:10.1016/j.cmet.2010.04.013
Kuznetsova, A., Brockhoff, P. B. and Christensen, R. H. B. (2017). lmerTest package: tests in linear mixed effects models. *J. Stat. Softw.* **82**, 26. doi:10.18637/jss.v082.i13
Lawson, H. A., Zayed, M., Wayhart, J. P., Fabbrini, E., Love-Gregory, L., Klein, S. and Semenkovich, C. F. (2017). Physiologic and genetic evidence links hemopexin to triglycerides in mice and humans. *Int. J. Obes.* **41**, 631-638. doi:10.1038/ijo.2017.19
Lee, Y. S., Choi, J. W., Hwang, I., Lee, J. W., Lee, J. H., Kim, A. Y., Huh, J. Y., Koh, Y. J., Koh, G. Y., Son, H. J. et al. (2010). Adipocytokine orosomucoid integrates inflammatory and metabolic signals to preserve energy homeostasis by resolving immoderate inflammation*. *J. Biol. Chem.* **285**, 22174-22185. doi:10.1074/jbc.M109.085464
Li, X., Wang, F., Xu, M., Howles, P. and Tso, P. (2017). ApoA-IV improves insulin sensitivity and glucose uptake in mouse adipocytes via PI3K-Akt Signaling. *Sci. Rep.* **7**, 41289. doi:10.1038/srep41289
Ling, J. and Thomas, C. (1967). The skin and hair of the southern elephant seal, (Mirounga Leonina (L.) II. pre-natal and early post-natal development and moulting. *Aust. J. Zool.* **15**, 349-365. doi:10.1071/ZO9670349
Lu, H., Cassis, L. A., Kooi, C. W. V. and Daugherty, A. (2016). Structure and functions of angiotensinogen. *Hypertens. Res.* **39**, 492-500. doi:10.1038/hr.2016.17
Martinez, B., Scheibner, M., Sonanez-Organis, J. G., Jaques, J. T., Crocker, D. E. and Ortiz, R. M. (2017). Increased sensitivity of thyroid hormone-mediated signaling despite prolonged fasting. *Gen. Comp. Endocrinol.* **252**, 36-47. doi:10.1016/j.ygcen.2017.07.023
Martinez, B., Khudyakov, J., Rutherford, K., Crocker, D. E., Gemmell, N. and Ortiz, R. M. (2018). Adipose transcriptome analysis provides novel insights into molecular regulation of prolonged fasting in northern elephant seal pups. *Physiol. Genomics* **50**, 495-503. doi:10.1152/physiolgenomics.00002.2018
Meex, R. C., Hoy, A. J., Morris, A., Brown, R. D., Lo, J. C., Burke, M., Goode, R. J., Kingwell, B. A., Kraakman, M. J., Febbraio, M. A. et al. (2015). Fetuin B is a secreted hepatocyte factor linking steatosis to impaired glucose metabolism. *Cell Metab.* **22**, 1078-1089. doi:10.1016/j.cmet.2015.09.023
Mohr, S. M., Bagriantsev, S. N. and Gracheva, E. O. (2020). Cellular, molecular, and physiological adaptations of hibernation: the solution to environmental challenges. *Annu. Rev. Cell Dev. Biol.* **36**, 315-338. doi:10.1146/annurev-cellbio-012820-095945
Ortiz, R. M., Crocker, D. E., Houser, D. S. and Webb, P. M. (2006). Angiotensin II and aldosterone increase with fasting in breeding adult male northern elephant seals (Mirounga angustirostris). *Physiol. Biochem. Zool.* **79**, 1106-1112. doi:10.1086/505996
Qu, J., Ko, C.-W., Tso, P. and Bhargava, A. (2019). Apolipoprotein A-IV: a multifunctional protein involved in protection against atherosclerosis and diabetes. *Cells* **8**, 319. doi:10.3390/cells8040319
Qu, J., Fourman, S., Fitzgerald, M., Liu, M., Nair, S., Oses-Prieto, J., Burlingame, A., Morris, J. H., Davidson, W. S., Tso, P. et al. (2021). Low-density lipoprotein receptor-related protein 1 (LRP1) is a novel receptor for apolipoprotein A4 (APOA4) in adipose tissue. *Sci. Rep.* **11**, 13289. doi:10.1038/s41598-021-92711-0
Revelle, W. (2019). *psych: Procedures for Psychological, Psychometric, and Personality Research*. Evanston, IL: Northwestern University.
Ritchie, M. E., Phipson, B., Wu, D., Hu, Y., Law, C. W., Shi, W. and Smyth, G. K. (2015). limma powers differential expression analyses for RNA-sequencing and microarray studies. *Nucleic Acids Res.* **43**, e47. doi:10.1093/nar/gkv007
Robinson, P. W., Costa, D. P., Crocker, D. E., Gallo-Reynoso, J. P., Champagne, C. D., Fowler, M. A., Goetsch, C., Goetz, K. T., Hassrick, J. L., Huckstadt, L. A. et al. (2012). Foraging behavior and success of a mesopelagic predator in the northeast Pacific Ocean: insights from a data-rich species, the northern elephant seal. *PLoS One* **7**, e36728. doi:10.1371/journal.pone.0036728
Rzucidlo, C. L., Sperou, E. S., Holser, R. R., Khudyakov, J. I., Costa, D. P. and Crocker, D. E. (2021). Changes in serum adipokines during natural extended fasts in female northern elephant seals. *Gen. Comp. Endocrinol.* **308**, 113760. doi:10.1016/j.ygcen.2021.113760
Sapolsky, R. M., Romero, L. M. and Munck, A. U. (2000). How do glucocorticoids influence stress responses? Integrating permissive, suppressive, stimulatory, and preparative actions. *Endocr. Rev.* **21**, 55-89. doi:10.1210/edrv.21.1.0389
Secor, S. M. and Carey, H. V. (2016). Integrative physiology of fasting. *Compr Physiol* **6**, 773-825. doi:10.1002/cphy.c150013
Slenter, D. N., Kutmon, M., Hanspers, K., Riutta, A., Windsor, J., Nunes, N., Mélius, J., Cirillo, E., Coort, S. L., Digles, D. et al. (2018). WikiPathways: a multifaceted pathway database bridging metabolomics to other omics research. *Nucleic Acids Res.* **46**, D661-D667. doi:10.1093/nar/gkx1064
Sramkova, V., Berend, S., Siklova, M., Caspar-Bauguil, S., Carayol, J., Bonnel, S., Marques, M., Decaunes, P., Kolditz, C.-I., Dahlman, I. et al. (2019). Apolipoprotein M: a novel adipokine decreasing with obesity and upregulated by calorie restriction. *Am. J. Clin. Nutr.* **109**, 1499-1510. doi:10.1093/ajcn/nqy331
Stacklies, W., Redestig, H., Scholz, M., Walther, D. and Selbig, J. (2007). pcaMethods–a bioconductor package providing PCA methods for incomplete data. *Bioinformatics* **23**, 1164-1167. doi:10.1093/bioinformatics/btm069
Struntz, D. J., McLellan, W. A., Dillaman, R. M., Blum, J. E., Kucklick, J. R. and Pabst, D. A. (2004). Blubber development in bottlenose dolphins (Tursiops truncatus). *J. Morphol.* **259**, 7-20. doi:10.1002/jmor.10154
Su, X. and Peng, D. (2020). The exchangeable apolipoproteins in lipid metabolism and obesity. *Clin. Chim. Acta* **503**, 128-135. doi:10.1016/j.cca.2020.01.015
Suzuki, M., Vazquez-Medina, J. P., Viscarra, J. A., Sonanez-Organis, J. G., Crocker, D. E. and Ortiz, R. M. (2013). Activation of systemic, but not local, renin-angiotensin system is associated with upregulation of TNF-alpha during prolonged fasting in northern elephant seal pups. *J. Exp. Biol.* **216**, 3215-3221. doi:10.1242/jeb.085225
Tift, M. S., Houser, D. S. and Crocker, D. E. (2011). High-density lipoprotein remains elevated despite reductions in total cholesterol in fasting adult male elephant seals (Mirounga angustirostris). *Comp. Biochem. Physiol. B Biochem. Mol. Biol.* **159**, 214-219. doi:10.1016/j.cbpb.2011.04.005
Vann, C. G., Osburn, S. C., Mumford, P. W., Roberson, P. A., Fox, C. D., Sexton, C. L., Johnson, M.-R., Johnson, J. S., Shake, J., Moore, J. H. et al. (2020). Skeletal muscle protein composition adaptations to 10 weeks of high-load

resistance training in previously-trained males. *Front. Physiol.* **11**, 259. doi:10.3389/fphys.2020.00259

Viscarra, J. A., Champagne, C. D., Crocker, D. E. and Ortiz, R. M. (2011). 5′AMP-activated protein kinase activity is increased in adipose tissue of northern elephant seal pups during prolonged fasting-induced insulin resistance. *J. Endocrinol.* **209**, 317-325. doi:10.1530/JOE-11-0017

Wang, F., Kohan, A. B., Lo, C.-M., Liu, M., Howles, P. and Tso, P. (2015). Apolipoprotein A-IV: a protein intimately involved in metabolism. *J. Lipid Res.* **56**, 1403-1418. doi:10.1194/jlr.R052753

Wei, X., Liu, X., Tan, C., Mo, L., Wang, H., Peng, X., Deng, F. and Chen, L. (2019). Expression and function of zinc-α2-glycoprotein. *Neurosci. Bull.* **35**, 540-550. doi:10.1007/s12264-018-00332-x

Weng, W. and Breslow, J. L. (1996). Dramatically decreased high density lipoprotein cholesterol, increased remnant clearance, and insulin hypersensitivity in apolipoprotein A-II knockout mice suggest a complex role for apolipoprotein A-II in atherosclerosis susceptibility. *Proc. Natl. Acad. Sci. USA* **93**, 14788-14794. doi:10.1073/pnas.93.25.14788

Wittwer, J. and Bradley, D. (2021). Clusterin and its role in insulin resistance and the cardiometabolic syndrome. *Front. Immunol.* **12**, 450. doi:10.3389/fimmu.2021.612496

Worthy, G. A. J., Morris, P. A., Costa, D. P. and Boeuf, B. J. L. (1992). Moult energetics of the northern elephant seal (Mirounga angustirostris). *J. Zool.* **227**, 257-265. doi:10.1111/j.1469-7998.1992.tb04821.x

Wright, T. J., Davis, R. W., Holser, R. R., Hückstädt, L. A., Danesi, C. P., Porter, C., Widen, S. G., Williams, T. M., Costa, D. P. and Sheffield-Moore, M. (2020). Changes in northern elephant seal skeletal muscle following thirty days of fasting and reduced activity. *Front. Physiol.* **11**, 564555. doi:10.3389/fphys.2020.564555

Yu, G., Wang, L.-G., Han, Y. and He, Q.-Y. (2012). clusterProfiler: an R Package for comparing biological themes among gene clusters. *OMICS* **16**, 284-287. doi:10.1089/omi.2011.0118

Zhang, Y., Shen, W., Li, J., Zheng, B., Lou, Z., Hosain, M. A., Qian, B. and Xue, L. (2021). Effect of fasting on protein metabolism in muscle tissue of Larimichthys crocea revealed by transcriptome and proteome. *J. Oceanol. Limnol.* **39**, 1972-1984. doi:10.1007/s00343-020-0273-5

Zhu, Q., Weng, J., Shen, M., Fish, J., Shen, Z., Coschigano, K. T., Davidson, W. S., Tso, P., Shi, H. and Lo, C. C. (2020). Apolipoprotein A-IV enhances fatty acid uptake by adipose tissues of male mice via sympathetic activation. *Endocrinology* **161**, bqaa042. doi:10.1210/endocr/bqaa042

Table S1. Age, date of sampling, mass, adiposity (adip.), and serum cortisol of adult female NES used in the study.

ID	age	early molt				late molt				early breeding			
		date	mass (kg)	adip.	cortisol (nM)	date	mass (kg)	adip.	cortisol (nM)	date	mass (kg)	adip.	cortisol (nM)
5572	5	5/01/16	324	0.362	55.8	6/07/16	231	0.335	746.7	2/01/17	394	0.345	462.0
9678	--	5/02/16	447	0.348	94.9	6/07/16	331	0.346	927.1	1/23/17	512	0.368	818.2
4448	6	5/12/16	384	0.309	40.8	6/16/16	277	--	997.7	--	--	--	--
6762	5	5/16/16	336	0.359	150.9	6/15/16	--	0.296	559.6	--	--	--	--
X410	7	5/30/16	394	0.330	500.7	6/27/16	303	0.287	4103.5	--	--	--	--
mean (s.d.)	5.75 (0.96)	--	397 (73)	0.342 (0.022)	173.3 (186.6)	--	273 (46)	0.316 (0.029)	1466.9 (1483.7)	--	453 (83)	0.356 (0.016)	640.1 (251.9)

Table S2. Plasma triglyceride (TG) and serum total cholesterol (TC), high-density lipoprotein cholesterol (HDL), and low-density lipoprotein/very low-density lipoprotein (LDL/VLDL) of adult female NES used in the study.

ID	early molt				late molt				early breeding			
	TG (mg/dl)	TC (mg/dl)	HDL (mg/dl)	LDL/ VLDL (mg/dl)	TG (mg/dl)	TC (mg/dl)	HDL (mg/dl)	LDL/ VLDL (mg/dl)	TG (mg/dl)	TC (mg/dl)	HDL (mg/dl)	LDL/ VLDL (mg/dl)
5572	27.8	317.2	197.6	141.5	28.5	293.9	197.2	106.8	60.7	325.6	174.4	138.3
9678	37.1	397.2	233.4	178.7	23.4	319.0	194.8	143.8	29.4	315.3	207.6	154.4
4448	40.8	390.2	229.6	186.0	17.7	332.1	216.8	117.5	--	--	--	--
6762	41.0	332.1	235.8	111.4	49.7	320.1	230.9	105.9	--	--	--	--
X410	43.0	362.5	266.0	129.9	49.2	319.2	202.4	124.1	--	--	--	--
mean (s.d.)	37.9 (6.1)	359.9 (35.0)	232.5 (24.3)	149.5 (32.0)	33.7 (14.9)	316.8 (14.0)	208.4 (15.2)	119.6 (15.5)	45.0 (22.1)	320.4 (7.3)	191.0 (23.5)	146.3 (11.4)

Table S3.

Click here to download Table S3

Table S4.

Click here to download Table S4

Table S5.

Click here to download Table S5